A Laboratory Dust Generator Applying Vibration to Soil Sample: Mineralogical Study and Compositional Analyses

Z. Qu, A. Trabelsi, R. Losno, F. Monna, S. Nowak, M. Masmoudi, J. -P. Quisefit

JGR Atmospheres

RESEARCH ARTICLE
10.1029/2019JD032224

Key Points:
- Compositional analysis using biplots and Aitchison distance is a valuable tool for chemical variation comparisons
- Dust aerosol can be extracted from soil using vibrations as well as wind friction
- Figures of merit of a new small size dust generator system for fast extraction of dust from parent soil

Supporting Information:
- Supporting Information S1

Correspondence to:
R. Losno,
losno@ipgp.fr

Citation:
Qu, Z., Trabelsi, A., Losno, R., Monna, F., Nowak, S., Masmoudi, M., & Quisefit, J.-P. (2020). A laboratory dust generator applying vibration to soil sample: Mineralogical study and compositional analyses. *Journal Geophysical Research: Atmospheres*, *125*, e2019JD032224. https://doi.org/10.1029/2019JD032224

Received 12 DEC 2019
Accepted 25 MAR 2020
Accepted article online 4 APR 2020

A Laboratory Dust Generator Applying Vibration to Soil Sample: Mineralogical Study and Compositional Analyses

Z. Qu[1,2], A. Trabelsi[3], R. Losno[1], F. Monna[4], S. Nowak[5], M. Masmoudi[3], and J.-P. Quisefit[2]

[1]Université de Paris, Institut de Physique du Globe de Paris, UMR CNRS 7154, Paris, France, [2]LISA-Université Paris Est Créteil, Université de Paris, UMR CNRS 7583, Créteil, Paris, France, [3]Faculté des Sciences de Sfax, Sfax University, Sfax, Tunisia, [4]ArtéHis-UMR CNRS 6298, Université de Bourgogne-Franche Comté, Dijon, France, [5]RX Facility, Department of Chemistry, Université de Paris, Paris, France

Abstract A laboratory study was carried out using a vibrating system (SyGAVib) to produce aerosols from four soils collected in the central Tunisian region around Sfax. The aim of this device is to mimic dust emission by natural wind erosion. Using compositional analysis, the dust produced was compared to (i) dust generated in a wind tunnel by the same soils, (ii) fine sieved and (iii) original bulk soils, and (iv) naturally occurring aerosol samples collected in the same area. The relative quartz content strongly decreases from bulk to fine soils, and again from fine soils to both wind tunnel and vibration-generated aerosols. Compositional data analysis (CoDA) clearly shows (i) a silica dilution effect in bulk soils, and (ii) that if silica is removed from the composition, the elemental compositions of fine soils and generated aerosols are similar but differ from bulk soils. Both aerosol generation methods produce material with chemical compositions that are also close to those measured in field-sampled aerosols, and the fine soil composition is much closer to that of field and laboratory aerosols than to the parent soil. Aerosols generated from soils in the laboratory, either using a vibrating system or a wind tunnel, can be used as surrogates of the particles collected directly in the field.

Plain Language Summary A laboratory study was carried out using a vibrating system (SyGAVib) to produce particles from four soils collected in the central Tunisian region around Sfax. The aim of this device is to mimic dust emission by natural wind erosion. The chemical composition of the dust produced was compared to another dust generator (a wind tunnel), fine-sieved soil, original bulk soils, and finally naturally occurring dust found in the same area. Both dust generators produce similar samples which look very different from bulk soils.

1. Introduction

Mineral dust is extensively studied because its emission due to wind erosion in arid and semiarid regions of the globe accounts for approximately 30% to 50% of the total aerosol injections in the troposphere (Andreae, 1995). Mineral dust emission by wind erosion can be driven by direct aerodynamic resuspension (Kjelgaard et al., 2004), saltation bombardment, and aggregate disintegration (Gomes et al., 1990). Only the finest particles can remain in suspension in the atmosphere and be transported over thousands of kilometers from their emission areas (Arimoto, 2001). Consequently, the chemical composition of transported soil-derived dust is related to the fine fraction of soil particles and the use of the bulk source soil chemical composition as a surrogate for the dust chemical composition may result in systematic biases.

Natural dust emission from a given source is strongly dependent on local meteorological conditions and is difficult or even impossible to isolate from advection coming from elsewhere. Artificial dust production in the field or laboratory is an alternative way to study the source of the soil dust. Gillette (1978) investigated dust emission by wind erosion using a straight-line wind tunnel laid on the ground and Alfaro and Gomes (1995) brought soil into a wind tunnel mounted in their laboratory. Although the wind tunnel directly simulates the natural wind erosion process under controlled wind conditions, it is difficult to use due to the large amount of soil that needs to be brought back to the laboratory. To work at a laboratory bench scale, Lafon et al. (2014) generated desert dust by shaking soil samples in an Erlenmeyer flask, Engelbrecht et al. (2016) blown fine soil in a closed cabinet, Salam et al. (2006) generated aerosol by vibrating soil samples using a

Table 1
Soil Characteristics Using the WRB Classification Derived From Dry Sieving With a Stainless Steel System

Soil name	El Attaya	El Hsar	Cherarda	Ghraïba
Location (WGS84)	34°44′N 11°18′E	34°42′N 11°09′E	35°22′N 10°10′E	34°24′N 10°18′E
Nature	oolitic limestone	continental silt	limestone bed	alluvium and wind sand
Soil Fraction (%)				
Coarse and medium sand (>200 μm)	30.0	44.2	35.9	69.1
Fine and ultrafine sand (between 63 and 200 μm)	61.5	48.2	59.9	29.0
Silt and clays (<63 μm)	8.5	7.6	4.2	1.9

Note. El Attaya and El Hsar are located on Kerkennah Island. The finest fraction contains aggregated silt and clay particles.

loudspeaker to study the ice nucleation efficiency, and Mendez et al. (2013) used a rotating drum. For further details regarding previous experiments see the extensive review on aerosol generation published by Gill et al. (2006). Note that some authors simply used fine sieved soils as dust analogs (Guieu et al., 2014).

Here, a new soil-derived dust generator has been developed. It is based on controlled vibration waves and requires a very small amount of bulk soil. The aim of this paper is to chemically compare the material produced by this new device with aerosols generated by the wind tunnel, fine mesh sieved soil, and original bulk soil. Chemical changes are evaluated using compositional analyses, a set of statistical tools especially designed for handling chemical compositions in a clear and concise manner (Monna et al., 2017; Pasquet et al., 2016).

2. Experimental Materials and Methods

2.1. Soil Sampling

Four different surface bulk soil samples of ≈10 kg each were collected in the Sfax region, Tunisia (see Table 1 for the sampling locations and physical properties). First, they were coarse sieved at 2 mm in the field (hereafter denoted as bulk soil, BS). In the laboratory, ≈100 g of each sample was dry sieved with a stainless-steel system to determine the texture (Table 1, supporting information Table S1). Approximately, 10 g of the fine soil fraction (FS) was also obtained by sieving enough bulk soil on a 56 μm nylon mesh. The remaining material was homogenous and coarse sieved at 2 mm and was then divided into 5–6 aliquots of ≈2 kg each for the wind tunnel aerosol generation experiments. From these aliquots, ≈100 g was collected and well-mixed. Between 3 and 5 fractions of about 300 mg were subsampled for further SyGAVib measurement for each soil, and ≈5 g for EDXRF analyses.

2.2. Aerosol Generation

Approximately 0.3 g of soil was placed into an open-top ≈20 ml polyethylene cup that was fixed on top of a loudspeaker (Figure 1). Vibrations from the loudspeaker (sine-wave frequency = 100 Hz) levitated the soil particles, while collisions broke up the largest aggregates, favoring the emission of fine particles. The dust generation cup was placed at the bottom center of an upright stainless steel cylinder measuring 125 mm in diameter. Two air inlets were positioned at the bottom of the tube; a third air inlet directed toward the top center of the soil container created a local turbulence, which improved the extraction of the particles. An external pump and an optical particle counter, with flow rates of 5.5 and 2.8 L min^{-1}, respectively, were connected to the top of the cylinder to maintain a constant upward air flow within the system. The total ascending flow rate was ≈8 L min^{-1}, providing a vertical air velocity of ≈1.1 cm s^{-1}. According to Stoke's steady state equations, and assuming spherical particles with a density of 2.2 g cm^{-3}, only particles smaller than ≈10 μm were carried up to the top of the cylinder. Particles were collected during 40 min on a polycarbonate membrane filter (32 mm in diameter, and with a pore size of 0.4 μm). The whole system was placed in a vertical laminar flow hood to prevent any external contamination.

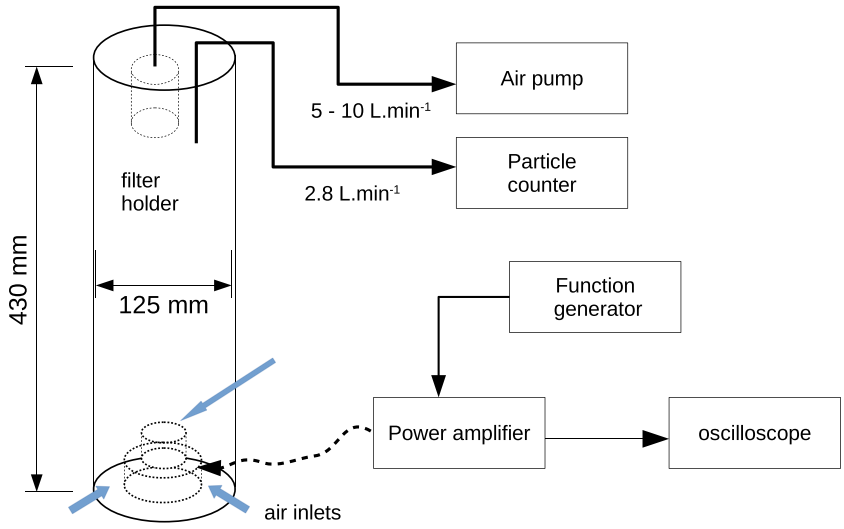

Figure 1. Diagram of the SyGAVib system.

The laboratory wind tunnel generator is extensively described in Alfaro and Gomes (1995) and Alfaro et al. (1997). In practice, ≈2 kg of soil were placed at the bottom of the wind tunnel ($30 \times 30 \times 400$ cm^3), and an air flow of ≈5 m s^{-1} was applied to generate aerosols for several minutes (2 to 15 depending on the generated dust concentration), This simulated wind speed induces a friction velocity large enough to produce saltation and simulates wind erosion with a process occurring under natural conditions. The generated aerosol was pumped at midheight (10 cm) through a 30 μm cutoff diameter decanter, as described in Alfaro (2008) and deposited on similar polycarbonate filter membrane as that used for the SyGAVib experiments.

For each soil origin, aerosol generation was replicated 5–6 times by the wind tunnel device and 3–5 times by the SyGAVib device. At least one replicate was loaded to the maximum dust amount for mineralogical determinations by X-ray diffraction (XRD), while the other filters were adequately loaded for further elemental analysis using X-ray fluorescence spectrometry (XRF).

2.3. Soil and Aerosol Analyses

Chemical analyses were performed on the bulk soil and fine soil (BS and FS, respectively) using energy dispersive X-ray fluorescence spectrometry (EDXRF, Epsilon, PANalytical). Aerosol filters obtained with the wind tunnel (WT) and the SyGAVib (Syg) system were analyzed directly on the membrane filter in thin layer conditions for aerosols (Losno et al., 1987). Soil samples were first finely ground in a tungsten carbide ball mill and 5 g of the fine powder was transformed into a pressed pellet with an addition of 0.9 g of wax for the EDXRF analyses. Soil pellets were then analyzed as infinite thickness layers using the Ominan® software, which deconvolves spectra from the background and from the line overlaps, and empirically corrects matrix effects. Except for SO_3 and Na_2O, the detection limit is several μg g^{-1} and below 10% of the measured values. The initial calibration was established using 13 certified reference materials from SARM (Nancy): Anorthosite AN - G, Basalt BE - N, Basalt BR, Bauxite BX - N, Diorite DR - N, Disthene (Kyanite) DT - N, Granite AC - E, Granite GA, Granite GS - N, Granite MA - N, Phlogopite Mica - Mg, Potash Feldspar FK - N, and Serpentine UB - N.

Mineralogical analyses were performed by XRD using an EMPYREAN (PANalytical) diffractometer equipped with a copper anode and a multichannel PIXCEL® detector. Crystalline mineral identification and quantification were obtained for the bulk and fine soils, as well as generated aerosols (by both the wind tunnel and SyGAVib devices) using the Highscore Plus 3.0 software and ICSD database (Inorganic Crystal Structure Database). The MAUD program (Material Analysis Using Diffraction) is a general diffraction program mainly based on the Rietveld method (Lutterotti et al., 1999) and is specifically used for the semiquantitative phase analysis in this work.

The aerosol size distribution was obtained from the six channels (>0.3, >0.5, >0.7, >1, >2 and >5 μm) provided by a MetOne 237B laser particle counter.

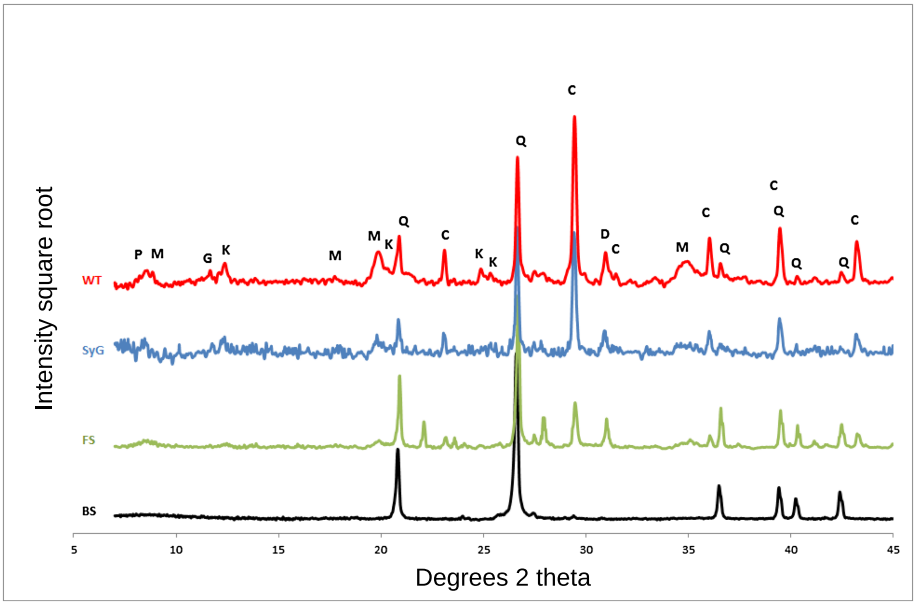

Figure 2. Diffractograms of the aerosols generated by the SyGAVib system and the wind tunnel from the Ghraiba soil. Each diffractogram intensity was rescaled to obtain the same average height on a square root scale. WT: wind tunnel, SyG: SyGaVib, FS: fine soil, BS: bulk soil; Q: quartz, D: dolomite, C: calcite, M: muscovite, K: kaolinite, P: palygorskite, G: gypsum. The diffractograms and semi-quantitative mineralogical composition of the other soils are provided in the supporting information (Figures S1 and S2 and Table S2).

2.4. Statistical Compositional Analysis

Data processing was performed using the free R software (R Core Team, 2018), specifically with the "compositions" package (van den Boogaart et al., 2014) which provides a set of functions (acomp and princomp) especially designed to process compositional data.

3. Results and Discussion

3.1. Structure and Crystalline Mineralogy

From the sieve analysis, sand exceeds 91% of the total mass for all soils (Tables 1 and S1); as a result, the soil samples are classed as sandy according to the common soil classification (Baize, 2000). Soil from Ghraiba is the sandiest (98%) and the least silty, whereas that from Kerkennah is the siltiest, with ≈8% of silt and clay. Different types of aggregates are generally observed in dry soils from arid and semiarid regions. These aggregates are either almost exclusively composed of very small individual particles (Alfaro et al., 1997), or of a "core" (most often a quartz grain) to which some small clay plates, or assemblages of plates, adhere (Engelbrecht et al., 2009, 2016; Rajot et al., 2003).

Figure 2 shows an example of the four diffractograms obtained for the Ghraiba soils and derived daughter samples. A strong decrease in the relative intensity of the quartz diffraction peaks is observed from bulk soil to generated aerosols, with a simultaneous increase in the peaks for clay and calcite, which are the major mineral crystalline phases. This quartz depletion from soil to dust was already observed by Caquineau (2002) on transported airborne Saharan dust samples collected at Cape Verde, Barbados, and Miami, and also by Engelbrecht et al. (2009) for resuspended aerosols from the Middle East. Sieving the bulk soil also decreases the relative quartz content, but to a lesser extent. Regardless of which device was used (SyGAVib or wind tunnel), the diffractograms for the generated aerosol samples are similar in terms of their pattern as well as their semiquantitative results (Figure 3), indicating a comparable mineralogical composition.

3.2. Aerosol Size Distribution

The size distribution, expressed as the number of particles, of the material produced by the SyGAVib device is consistent all throughout the experiments; this is apparently not the case with the wind tunnel

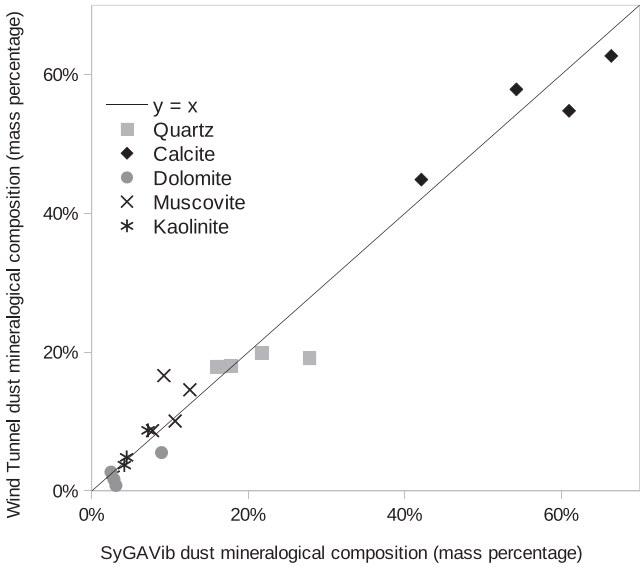

Figure 3. Comparison of the semiquantitative analyses of the selected minerals in wind tunnel experiments (WT, y axis) versus Sygavib experiments (Syg, x axis) for the four parent soils aerosol samples. The line $y = x$ have been drawn.

experiments as the first replicate is notably enriched in the finest particles (0.3–0.5 μm channel in Figure 4). Given that this finest fraction only accounts for less than 1% of the total aerosol mass (Figure S3), this should have little influence on the overall composition of the collected aerosol, at least on the major and minor elements or phases. Both aerosol generation methods present a maximum number of particles within the 2–5 μm fraction, but particles tend to be larger when they are produced by the wind tunnel compared with SyGAVib (Figure 4).

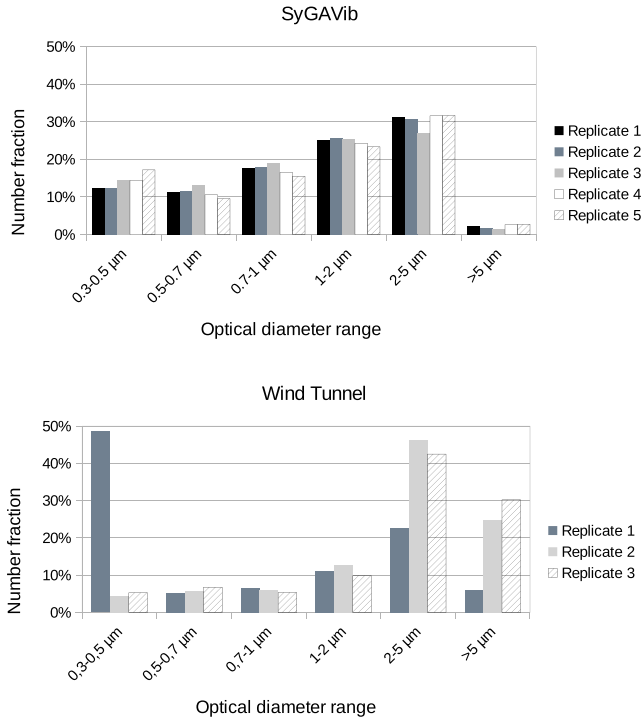

Figure 4. Size distributions (in terms of particles number) of the replicates of the dust generated by the SyGAVib system (n = 5, 40 min each) and wind tunnel (n = 3, 3 min each) averaged for the total duration of each replicate for the Cherarda soil (top) SyGAVib and (bottom) WT experiments). Size distribution in terms of mass fraction is provided in the supporting information, Figure S3.

Table 2
Chemical Composition of Soils and Aerosols Expressed as Oxide Percent

	CaO	SiO_2	Al_2O_3	Fe_2O_3	MgO	K_2O	Na_2O	TiO_2	SrO	MnO	SO_3
Attaya_BS	13	78	2.7	1.4	1.2	1.1	0.7	0.29	0.08	0.014	0.3
Attaya_FS	28	45	9.3	5.0	3.7	2.3	1.5	0.90	0.14	0.052	2.1
Attaya_Syg	34	32	8.8	5.1	3.7	2.9	2.0	0.68	0.19	0.063	7.5
Attaya_WT	36	29	8.1	5.7	3.2	2.9	1.9	0.73	0.20	0.070	7.9
Cherrarda_BS	3.0	89	4.0	1.4	0.7	1.1	0.06	0.24	0.009	0.009	<0.1
Cherrarda_FS	18	59	11	5.1	2.3	2.3	0.22	0.96	0.045	0.048	0.2
Cherrarda_Syg	31	43	13	6.0	2.7	2.5	0.18	0.83	0.050	0.072	0.3
Cherrarda_WT	33	39	12	7.6	3.0	3.0	0.16	0.96	0.068	0.091	0.5
Ghraiba_BS	0.7	96	1.9	0.4	0.41	0.5	0.05	0.11	0.004	0.0039	0.15
Ghraiba_FS	18	60	8.8	4.5	3.0	2.2	0.39	1.15	0.053	0.045	0.7
Ghraiba_Syg	22	49	14	5.1	3.4	2.7	0.36	0.91	0.063	0.079	1.7
Ghraiba_WT	18	47	15	6.1	4.3	2.9	0.37	0.91	0.061	0.091	3.1
Hsar_BS	9.5	84	2.9	1.5	0.84	0.7	0.07	0.19	0.037	0.008	<0.1
Hsar_FS	31	49	8.9	4.6	3.0	2.0	0.25	0.89	0.079	0.035	0.3

Note. The abbreviations Syg, WT, FS, and BS stand for SyGAVib, wind tunnel, Fine Soil, and Bulk Soil, respectively. The Syg and WT aerosol samples correspond to the average of the replicates.

3.3. Chemical Composition

The elemental compositions expressed as oxides: SiO_2, Al_2O_3, Fe_2O_3, Ca_O, MgO, K_2O, Na_2O, TiO_2, SrO, MnO, and SO_3, were measured and averaged for all sample types (Table 2 and the measurement dispersion is reported in Table S3 in the supporting information).

The elemental ratios of the generated aerosols and fine soils over their corresponding bulk soils were calculated for each soil sample (see Figure 5 for the Cherrarda samples, and Figure S2 in the supporting information for the other soils). SiO_2 appears to be systematically depleted in all treatments that include sieving and generated aerosols, while all the other elements are enriched (their ratios are much higher than 1), as already pointed out in previous studies (Acosta et al., 2009; Schütz & Rahn, 1982). This is particularly obvious in the Ghraiba samples, which exhibited the highest silica content. This behavior can easily be explained by a more or less pronounced diluting effect of SiO_2.

This is fully coherent with the larger amount of quartz already identified via XRD analysis in bulk soils, and with the mineralogical changes observed after aerosol generation. As additional proof, when the elemental composition ratios were calculated without SiO_2 (considering the sum of all remaining elements as being equal to 100%), all elemental composition ratios tended toward unity (Figure 6). Although the influence of

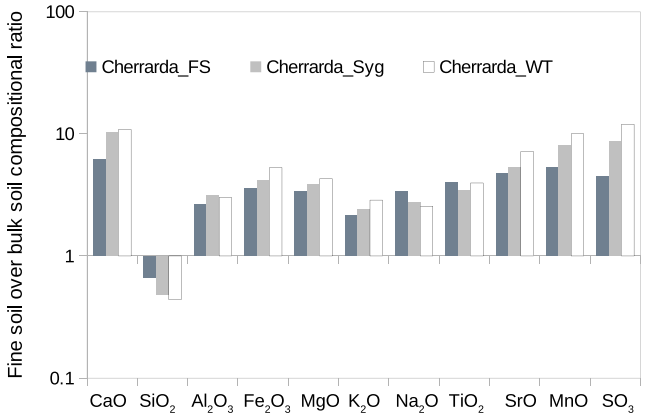

Figure 5. Compositional ratios of generated aerosol (Syg for SyGaVib, WT for wind tunnel) and fine soil (FS) over bulk soil for Cherrarda on a logarithmic scale.

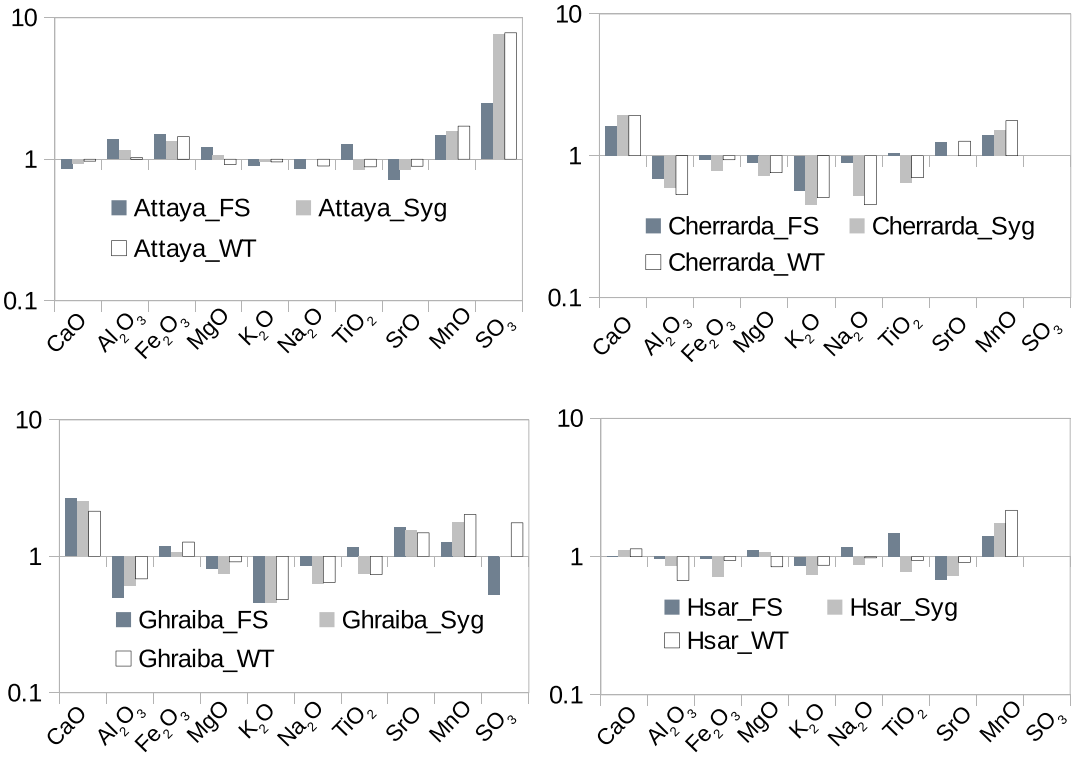

Figure 6. Compositional ratios of generated aerosol (Syg for SyGaVib, WT for wind tunnel) and fine soil (FS) over bulk soil for Cherrarda, excluding the silica contribution on a logarithmic scale.

SiO_2 is clear enough to be interpreted in a straightforward manner, it is more difficult to evaluate the extent to which the elemental composition has been modified by sieving or by aerosol generation, and to compare the results obtained between them after treatment.

Principal component analysis (PCA) is often successfully used to explore the internal structure of a geochemical data set (e.g., Engelbrecht & Jayanty, 2013), using a correlation matrix of the raw concentrations. However, it must be mentioned that if a strong diluting agent is present, such as quartz, strong spurious correlations may appear, due to the interdependence of the remaining components (Chayes, 1960). To circumvent this drawback related to the closed nature of any such data set, Aitchison (1986) developed a set of transformations and proposed a procedure to specifically treat this topic. In the following, centered log-ratio (clr) transformed data are used as inputs for a compositional PCA (see van den Boogaart et al., 2014; Pasquet et al., 2016 for details), instead of raw concentrations (oxides in this case). The data set can then be explored using a compositional biplot. This representation expresses the relative variation of a multivariate data set by projection onto a plane (Aitchison & Greenacre, 2002). Similarly to Gabriel (1971) classic biplot, samples and variables can be depicted together. However, the arrows formed by the variables cannot be interpreted directly. Only links between two arrow heads (i.e., the projection of the variables) are meaningful, and approximate the standard deviations of the log ratios of these variables. The angle cosines between the links estimate the correlations between two log ratios (for more details, see Aitchison & Greenacre, 2002; van den Boogaart & Tolosana-Delgado, 2013). A compositional biplot can therefore be used to examine elementary ratios (actually pairwise log ratios) in individuals, and not their level of concentrations, as observed in Gabriel's biplot. Note that absolute concentration values are lost with this treatment. Individual components cannot be interpreted when taken separately, similarly to Gabriel's classic biplot. Only log ratios between components make sense. The use of log ratios implies that elements close to the detection limit may lead to a very unstable response, modifying the complete biplot representation. As a consequence, these elements should be excluded from statistical analysis. This is the reason why SO_3 has been discarded here.

Figure 7 is a biplot presenting the results of the compositional data analyses on all parent and daughter samples with a very large dispersion of the log ratios; in the diagram, it can be observed that BS, FS, Syg, and WT are well spread out along the SiO_2 axis (demarcated by a red arrow). The second main split involves log

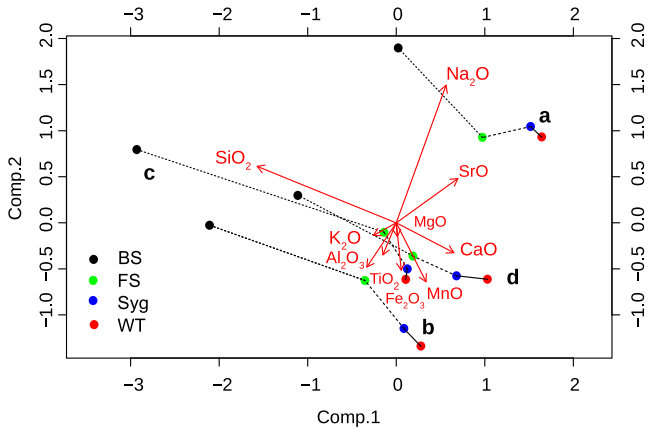

Figure 7. Compositional biplot including bulk and fine soils, and generated aerosol. Together Component 1 and Component 2 account for 86% of the total variance (56% and 30%, respectively). (a) Attaya, (b) Cherrarda, (c) Ghraiba, (d) Hsar. The solid line links the wind tunnel and SyGAVib-generated aerosol from the same soil type, the dashed line links the SyGAVib and fine soils of the same soil type.

ratios including sodium. It discriminates between the origins of the sample parent soils, but not the nature of the sample (BS, FS, WT, or Syg). This type of graph presents clearer and more concise compositional variations than the bar graphs shown in Figures 5 and 6, where the dilution effect of silica can be seen but not the role of sodium. As mentioned above, the physical distance between two points is equivalent to a compositional distance. By removing the influence of silica dilution and sodium soil discrimination, the bulk soil chemical composition remains clearly different from that of fine sieved soils, or generated aerosols, with no clear specific contribution of one given element (Figure 8). For each parent soil, the SyGAVib, wind tunnel, and fine soil generation methods are found relatively close together on the biplot diagram and thereby show similar compositions. However there were slightly more similarities between the two generated aerosols. The cutoff diameter, ranging from 56 μm for fine soil to 30 and 10 μm, respectively, for WT and Syg aerosol generations, does not have a strong effect on the chemical composition of the resulting material, when calculated without silica or sodium. When silica and sodium are excluded, fine sieved soils exhibit the same elemental ratios than aerosols produced with Sygavib or wind tunnel.

3.4. Comparisons With Field-Sampled Aerosols

Natural airborne aerosols have been collected and measured on Kerkennah Island, close to the bulk soil sampling locations, over a 1 year period in 2010 and 2011. Sampling was performed on a mast 2 m above the roof of a three levels building in a free area using the same filtration system and the same filters (Trabelsi et al., 2016). The Na_2O, MgO, and K_2O contents of these aerosols were much higher than those of the soils

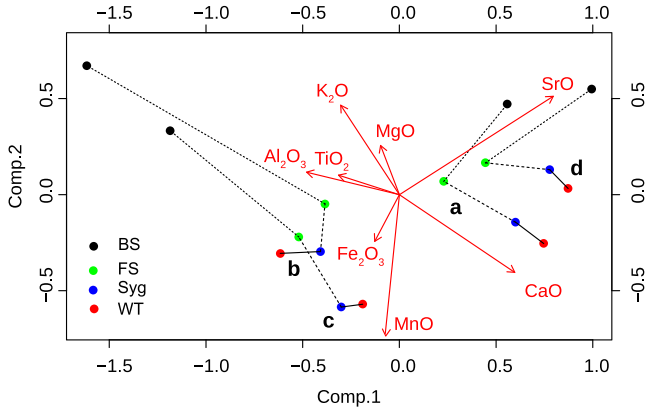

Figure 8. Compositional biplot including bulk and fine soils, and generated aerosol excluding the silica and sodium contribution. The solid line links the wind tunnel and SyGAVib-generated aerosol from the same soil type, the dashed line links the SyGAVib and fine soils of the same soil type. Together Component 1 and Component 2 account for 86% of the total variance (70% and 16%, respectively). (a) Attaya, (b) Cherrarda, (c) Ghraiba, (d) Hsar.

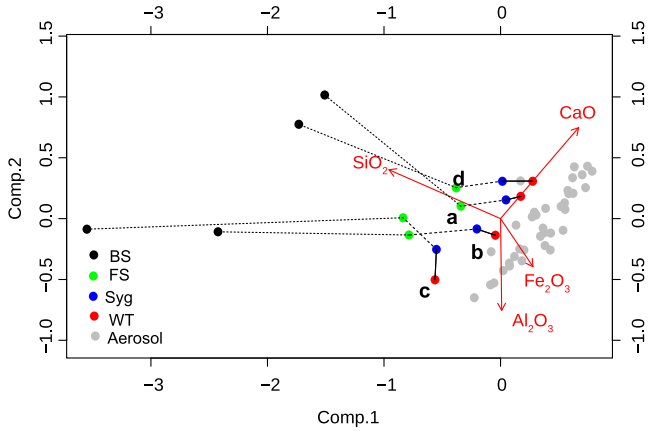

Figure 9. Compositional biplot of the soil, laboratory-generated aerosols and field aerosols except in winter. Component 1 and Component 2 account for 98% of the variance, with 84% for Component 1. (a) Attaya, (b) Cherrarda, (c) Ghraiba, (d) Hsar. Lines have the same meaning as in the Figures 7 and 8. Aerosol data are from Trabelsi et al. (2016).

and derived aerosols measured in the present study, due to a large contribution of sea salt aerosols, especially in winter. To assess the soil contribution to aerosols, these three elements were not considered, and samples collected in winter were removed. TiO_2, MnO, and SrO were not measured in the field aerosols. A new compositional biplot including bulk and fine soils, laboratory-generated aerosols, and field-sampled aerosols was produced using CaO, SiO_2, Al_2O_3, and Fe_2O_3 which are shared by both studies (Figure 9). Field-sampled aerosols were similar to both SyGAVib and wind tunnel aerosols, and quite different from bulk soils, due to the variation in the silica content, while fine soils were more similar to the aerosol samples than to the parent soils. In this case, aerosols generated by both the SyGAVib and wind tunnel device are approaching close to the airborne crustal aerosols collected in the field.

4. Conclusions

Using the new aerosol generation system by vibration (SyGAVib), it was possible to extract a fine soil fraction (<10 μm) with a chemical and mineralogical composition similar to wind-generated aerosols for a given soil. It is worth mentioning that full details concerning setup and comparison with the other methods are provided, so that any researcher will be able to reproduce the process described here in other environmental conditions. This vibration system, which is much smaller than a wind tunnel, can be installed on a laboratory bench at a low cost. This method does not require large amounts of parent soil (≈0.5 g), it gives a high collection yield, insures a clean sample without ambient air contamination, and it is easy to use. The fine fraction (<56 μm) of the soil is therefore a good substitute for a generated aerosol, at least when it is enough to simply work with internal elemental ratios excluding silica.

Acknowledgments
The full data set used to write this paper can be found in the supporting information and also in the AERIS database (https://doi.org/10.6096/DV/CGVYXC). We thank Sara Mullin for correcting the English language content and G. Brissebrat for the AERIS database. We are grateful to the anonymous reviewers whose judicious comments have improved the manuscript.

References

Acosta, J. A., Cano, A. F., Arocena, J. M., Debela, F., & Martínez-Martínez, S. (2009). Distribution of metals in soil particle size fractions and its implication to risk assessment of playgrounds in Murcia City (Spain). *Geoderma*, *149*(1-2), 101–109. https://doi.org/10.1016/j.geoderma.2008.11.034

Aitchison, J. M. (1986). *The statistical analysis of compositional data*. London: Chapman and Hall.

Aitchison, J., & Greenacre, M. (2002). Biplots of compositional data. *Journal of the Royal Statistical Society: Series C (Applied Statistics)*, *51*(4), 375–392. https://doi.org/10.1111/1467-9876.00275

Alfaro, S. C. (2008). Influence of soil texture on the binding energies of fine mineral dust particles potentially released by wind erosion. *Geomorphology*, *93*(3-4), 157–167. https://doi.org/10.1016/j.geomorph.2007.02.012

Alfaro, S. C., Gaudichet, A., Gomes, L., & Maillé, M. (1997). Modeling the size distribution of a soil aerosol produced by sandblasting. *Journal of Geophysical Research*, *102*(D10), 11,239–11,249. https://doi.org/10.1029/97JD00403

Alfaro, S. C., & Gomes, L. (1995). Improving the large-scale modeling of the saltation flux of soil particles in presence of nonerodible elements. *Journal of Geophysical Research*, *100*(D8), 16,357. https://doi.org/10.1029/95JD01281

Andreae, M. O. (1995). 10. Climatic effects of changing atmospheric aerosol levels, *Future climates of the world: A modelling perspective* (pp. 341–392). Amsterdam; New York: Elsevier. Retrieved from https://www.elsevier.com/books/future-climates-of-the-world/henderson-sellers/978-0-444-89322-2

Arimoto, R. (2001). Eolian dust and climate: relationships to sources, tropospheric chemistry, transport and deposition. *Earth-Science Reviews*, *54*(1-3), 29–42. https://doi.org/10.1016/S0012-8252(01)00040-X

Caquineau, S. (2002). Mineralogy of Saharan dust transported over northwestern tropical Atlantic Ocean in relation to source regions. *Journal of Geophysical Research*, *107*(D15), 4251. https://doi.org/10.1029/2000JD000247

Chayes, F. (1960). On correlation between variables of constant sum. *Journal of Geophysical Research*, *65*(12), 4185–4193. https://doi.org/10.1029/JZ065i012p04185

Engelbrecht, J. P., & Jayanty, R. K. M. (2013). Assessing sources of airborne mineral dust and other aerosols, in Iraq. *Aeolian Research*, *9*, 153–160. https://doi.org/10.1016/j.aeolia.2013.02.003

Engelbrecht, J. P., McDonald, E. V., Gillies, J. A., "Jay" Jayanty, R. K. M., Casuccio, G., & Gertler, A. W. (2009). Characterizing mineral dusts and Other Aerosols from the Middle East - Part 2: Grab Samples and Re-Suspensions. *Inhalation Toxicology*, *21*(4), 327–336. https://doi.org/10.1080/08958370802464299

Engelbrecht, J. P., Moosmüller, H., Pincock, S., Jayanty, R. K. M., Lersch, T., & Casuccio, G. (2016). Technical note: Mineralogical, chemical, morphological, and opticalinterrelationships of mineral dust re-suspensions. *Atmospheric Chemistry and Physics*, *16*(17), 10,809–10,830. https://doi.org/10.5194/acp-16-10809-2016

Gabriel, K. R. (1971). The biplot graphic display of matrices with application to principal component analysis. *Biometrika*, *58*(3), 453–467. https://doi.org/10.1093/biomet/58.3.453

Gill, T. E., Zobeck, T. M., & Stout, J. E. (2006). Technologies for laboratory generation of dust from geological materials. *Journal of Hazardous Materials*, *132*(1), 1–13. https://doi.org/10.1016/j.jhazmat.2005.11.083

Gillette, D. (1978). Tests with a portable wind tunnel for determining wind erosion threshold velocities. *Atmospheric Environment (1967)*, *12*(12), 2309–2313. https://doi.org/10.1016/0004-6981(78)90271-8

Gomes, L., Bergametti, G., Coudé-Gaussen, G., & Rognon, P. (1990). Submicron desert dusts: A sandblasting process. *Journal of Geophysical Research*, *95*(D9), 13,927. https://doi.org/10.1029/JD095iD09p13927

Guieu, C., Dulac, F., Ridame, C., & Pondaven, P. (2014). Introduction to project DUNE, a DUst experiment in a low Nutrient, low chlorophyll Ecosystem. *Biogeosciences*, *11*(2), 425–442. https://doi.org/10.5194/bg-11-425-2014

Kjelgaard, J. F., Chandler, D. G., & Saxton, K. E. (2004). Evidence for direct suspension of loessial soils on the Columbia Plateau. *Earth Surface Processes and Landforms*, *29*(2), 221–236. https://doi.org/10.1002/esp.1028

Lafon, S., Alfaro, S. C., Chevaillier, S., & Rajot, J. L. (2014). A new generator for mineral dust aerosol production from soil samples in the laboratory: GAMEL. *Aeolian Research*, *15*, 319–334. https://doi.org/10.1016/j.aeolia.2014.04.004

Losno, R., Bergametti, G., & Mouvier, G. (1987). Determination of optimal conditions for atmospheric aerosol analysis by X-ray fluorescence. *Environmental Technology Letters*, *8*(1-12), 77–86. https://doi.org/10.1080/09593338709384465

Lutterotti, L., Matthies, S., & Wenk, H. R. (1999). MAUD: A friendly Java program for material analysis using diffraction. *IUCr: Newsletter of the CPD*, *21*, 14–15.

Mendez, M. J., Panebianco, J. E., & Buschiazzo, D. E. (2013). A new dust generator for laboratory dust emission studies. *Aeolian Research*, *8*, 59–64. https://doi.org/10.1016/j.aeolia.2012.10.007

Monna, F., Marques, A. N., Guillon, R., Losno, R., Couette, S., Navarro, N., et al. (2017). Perturbation vectors to evaluate air quality using lichens and bromeliads: A Brazilian case study. *Environmental Monitoring and Assessment*, *189*(11), 566. https://doi.org/10.1007/s10661-017-6280-0

Pasquet, C., Le Monier, P., Monna, F., Durlet, C., Brigaud, B., Losno, R., et al. (2016). Impact of nickel mining in New Caledonia assessed by compositional data analysis of lichens. *SpringerPlus*, *5*(1), 2022. https://doi.org/10.1186/s40064-016-3681-4

R Core Team (2018). *R: A language and environment for statistical computing*. Vienna, Austria: R Foundation for Statistical Computing. Retrieved from http://www.R-project.org/

Rajot, J. L., Alfaro, S. C., Gomes, L., & Gaudichet, A. (2003). Soil crusting on sandy soils and its influence on wind erosion. *Catena*, *53*(1), 1–16. https://doi.org/10.1016/S0341-8162(02)00201-1

Salam, A., Lohmann, U., Crenna, B., Lesins, G., Klages, P., Rogers, D., et al. (2006). Ice nucleation studies of mineral dust particles with a new continuous flow diffusion chamber. *Aerosol Science and Technology*, *40*(2), 134–143. https://doi.org/10.1080/02786820500444853

Schütz, L., & Rahn, K. A. (1982). Trace-element concentrations in erodible soils. *Atmospheric Environment (1967)*, *16*(1), 171–176. https://doi.org/10.1016/0004-6981(82)90324-9

Trabelsi, A., Masmoudi, M., Quisefit, J. P., & Alfaro, S. C. (2016). Compositional variability of the aerosols collected on Kerkennah Islands (central Tunisia). *Atmospheric Research*, *169*, 292–300. https://doi.org/10.1016/j.atmosres.2015.10.018

van den Boogaart, K. G., & Tolosana-Delgado, R. (2013). *Analyzing compositional data with R*. Heidelberg: Springer. (OCLC: ocn827083643.

van den Boogaart, K. G., Tolosana-Delgado, R., & Bren, M. (2014). compositions: Compositional data analysis. R package version 1.40-1. Retrieved from https://CRAN.R-project.org/package=compositions